Research Article

Synthesis and Antimicrobial Assessment of Fe³⁺ Inclusion Complex of *p-tert*-Butylcalix[4]arene Diamide Derivative

Anwar Ali Chandio,[1] Ayaz Ali Memon,[1] Shahabuddin Memon,[1] Fakhar N. Memon,[2] Qadeer Khan Panhwar [D],[3] Fatih Durmaz,[4] Shafi Muhammad Nizamani,[1] and Nazir Ahmed Brohi[5]

¹National Centre of Excellence in Analytical Chemistry, University of Sindh, Jamshoro, Pakistan
²Department of Chemistry, University of Karachi, Karachi 75270, Pakistan
³Dr. M. A. Kazi, Institute of Chemistry, University of Sindh, Jamshoro, Pakistan
⁴Department of Chemistry, Selçuk University, 42031 Konya, Turkey
⁵Department of Microbiology, University of Sindh, Jamshoro, Pakistan

Correspondence should be addressed to Qadeer Khan Panhwar; qadeer.panhwar@usindh.edu.pk

Present study deals with the synthesis of the *p-tert*-butylcalix[4]arene diamide derivative as ligand (L) and its Fe^{3+} complex, followed by its characterization using TLC and FT-IR, while UV-Vis and Job's plot study were performed for complex formation. Antimicrobial activity of the derivative (L) and its metal complex was carried out by the disc diffusion method against bacteria (*Escherichia coli* and *Staphylococcus albus*) and fungi (*R. stolonifer*). Different concentrations of the derivative (L) (6, 3, 1.5, 0.75, and 0.37 μg/mL) and its Fe^{3+} complex were prepared, and Mueller–Hinton agar was used as the medium for the growth of microorganisms. Six successive dilutions of the derivative (L) and Fe^{3+} complex were used against microorganisms. Two successive dilutions (6 and 3 μg/mL) of the derivative (L) showed antibacterial action against both Gram-positive and Gram-negative bacteria. In addition, three successive dilutions (6, 3, and 1.5 μg/mL) of the derivative (L) showed antifungal activity. However, all of six dilutions of the Fe^{3+} complex showed antimicrobial activity. Derivative (L) showed 3 and 1.5 μg/mL minimum inhibitory concentrations (MIC) against bacteria and fungi, respectively. On the contrary, its Fe^{3+} complex showed 0.37 μg/mL value of MIC against bacteria and fungi. Hence, Fe^{3+} complex of the derivative (L) was found to be a more effective antimicrobial agent against selected bacteria and fungi than the diamide derivative (L).

1. Introduction

During the past thirty years, calixarenes have been successfully merged into different fields because of their remarkable architectural distinctiveness. Sufficient literature has been published by researchers in which various applications of calixarenes have been explored like in catalysis, sensor technology, HPLC as the stationary phase, membrane technology, enzyme mimetic, chiral separation, nonlinear optics, and ion selective study and also as antimicrobial agents [1–6].

On the basis of their low mammalian toxicity, calixarenes were reported to have widespread applications in the field of pharmaceutical and biological sciences [7–9]. A group of researchers first time published research on antibacterial action of calixarenes. In their research, calixarene-based compounds were used against tuberculosis and mycobacteriosis models [10]. Another group of researchers showed the antibacterial activity of vancomycin-modified calix[4]arenes. They explored their synthesized compounds for the antimicrobial activity against bacteria, i.e., *Bacillus cereus, Staphylococcus epidermidis*, and *Staphylococcus aureus* [11]. In 2006, researchers designed novel antifungal agents hybrids of calix[4]arene and *amphotericin B* [12]. They observed that the antifungal action of both compounds

was either superior or equivalent to *amphotericin B*. The calixarene-based derivatives also proved to be excellent antifungal agents against selected fungi [13]. Recently, in 2012, the bioactivity assessment of water-soluble calix[4] arene derivatives was performed [6]. The compound showed good antimicrobial activity against selected microorganisms. Recently, some calix[4]arene-based diamide compounds as well as the Cu^{2+} complex were explored for antimicrobial activity [14].

The current study addresses the synthesis and characterization of the diamide derivative of *p-tert*-butylcalix[4] arene (L) and its Fe^{3+} complex and the assessment of relative antimicrobial studies of ligand and its complex.

2. Materials and Methods

Gallenkamp (UK) model was used to check the melting points on a M.F.B. 595.01 M, using conserved capillary tubes. FT-IR spectrophotometer (Thermo Nicollet AVATAR 5700) was also used (in the range 4000 to 400 cm^{-1}) by applying the KBr pellet method. CHNS instrument model Flash EA 1112 elemental analyzer (20090. Rodano, Milan, Italy) was used for elemental analysis. PerkinElmer (Shelton, CT06484, USA) Lambda-35 double-beam spectrophotometer was used for UV-Vis analysis, and standard 1.00 cm quartz cells were used.

Analytical grade chemicals were used without further purification. They were obtained from different sources: Merck (Darmstadt, Germany), Alfa Aesar (Germany), and Sigma (St. Louis, MO, USA). Plates (obtained from Merck), precoated with silica gel, were used for thin layer chromatography analysis. Glass apparatus was carefully cleaned and washed with 5 M nitric acid and subsequently with deionized water prior to use. Millipore Milli-Q Plus water purification system (ELGA Model CLASSIC UVF, UK) was used to obtain deionized water for the preparation of aqueous solutions. For the antimicrobial activity, culture medium was obtained from Oxoid Ltd, Basingstoke, Hampshire, England (Batch no. CM0337).

2.1. Experimental Scheme.
The sequential scheme for the present study is given in Figure 1.

2.2. Synthesis.
Compounds **1** and **2** were synthesized by the reported methods [15, 16]. Derivative (L) and its metal complex were synthesized according to the procedure depicted below.

Synthesis of the derivative (L) by the modified method was carried out by adding 1 mmol of compound (**2**) in 15 mL of chloroform and stirred for 5–10 minutes at room temperature. 50 mL solution of ethanolamine and methanol (1 : 3 v : v) was added dropwise to a flask containing compound (**2**), and the reaction was kept on stirring at room temperature. After 48 hours, white gummy material appeared, and the solvent was removed *via* the rotary evaporator. The remaining residue was dissolved in methanol, and distilled water was added into it; after vigorous shaking, white precipitates appeared which were

filtered and dried. Recrystallization in mixture of solvents (CH_2Cl_2 and CH3OH) gave white crystals, and the yield was 69.89% [17]. Derivative (L) was characterized with FT-IR and elemental.

2.3. UV-Spectroscopic Measurements.
Complexation study was carried out by using appropriate concentrations of the derivative (L) and metal cations. Stock solution of the derivative (L) (2.6×10^{-3} M) was prepared in 10 mL ethanol, which was further diluted to 100 mL (2.58×10^{-5} M) in ethanol. This method was used for spectroscopic analysis of the derivative (L). Using absorption cell of 1 cm, 10 equivalents of the essential metals were measured. 2 mL of the derivative (L) (2.6×10^{-5} M) and 2 mL of metal salts (2.6×10^{-4} M) were mixed together in 5 mL glass test tubes separately. Spectral response of the derivative (L) before and after the mixing of metals was recorded.

2.4. Determination of Complex Stoichiometry.
Stoichiometric ratio of the derivative (L) and metal (Fe^{3+}) was determined using Job's plot method. For this method, equimolar solutions (2.6×10^{-5} M) of both host and guest were added to each other in 1 : 9 to 9 : 1 varying ratios [18, 19].

2.5. Synthesis of Fe^{3+} Complex.
Iron complex was prepared according to Job's plot. The saturated solution of ligand was separately prepared followed by addition of stoichiometric amount of metal ions into the ligand solution. Subsequently, the solution was stirred at normal temperature for 24 hours. Finally, the solvent was evaporated, and the bright crystals obtained were dried in a vacuum oven. Complex was characterized with FT-IR and elemental analysis.

2.6. Microbial Study.
The modified disc diffusion method of Kirby–Bauer [20] was used to check the *in vitro* antimicrobial activity of the derivative (L) and its Fe^{3+} complex. With the help of American Type Culture Collection (ATCC), antimicrobial activity was studied against different microorganisms. The growth of microorganism species including bacteria and a fungus was carried out using the *Mueller–Hinton agar* (MHA) medium. Under the instructions of manufacturer, the culture medium was prepared and used. To check the antimicrobial activity of the derivative (L) and its Fe^{3+} complex, five successive dilutions 6, 3, 1.5, 0.75, and 0.37 (μg/mL) were prepared in absolute ethanol. Discs used were of Whatman No. 3 (Filter paper discs) with a diameter size of 6 mm. They were soaked in each prepared dilutions for a short period of time, and then under sterile circumstances, discs were dried (to get rid of residual solvent) at room temperature. After that, the discs were placed on microbial agar plates (made in streaking fashion) and incubated at 37°C for 24 hours (for bacteria) and 48 hours (for fungi). At the end of incubation period, the antimicrobial activity of compounds against each microbial species was recorded by measuring the zone of the inhibition diameter in millimeter (mm), and MIC levels were calculated. The tests were carried out in triplicate as suggested [21].
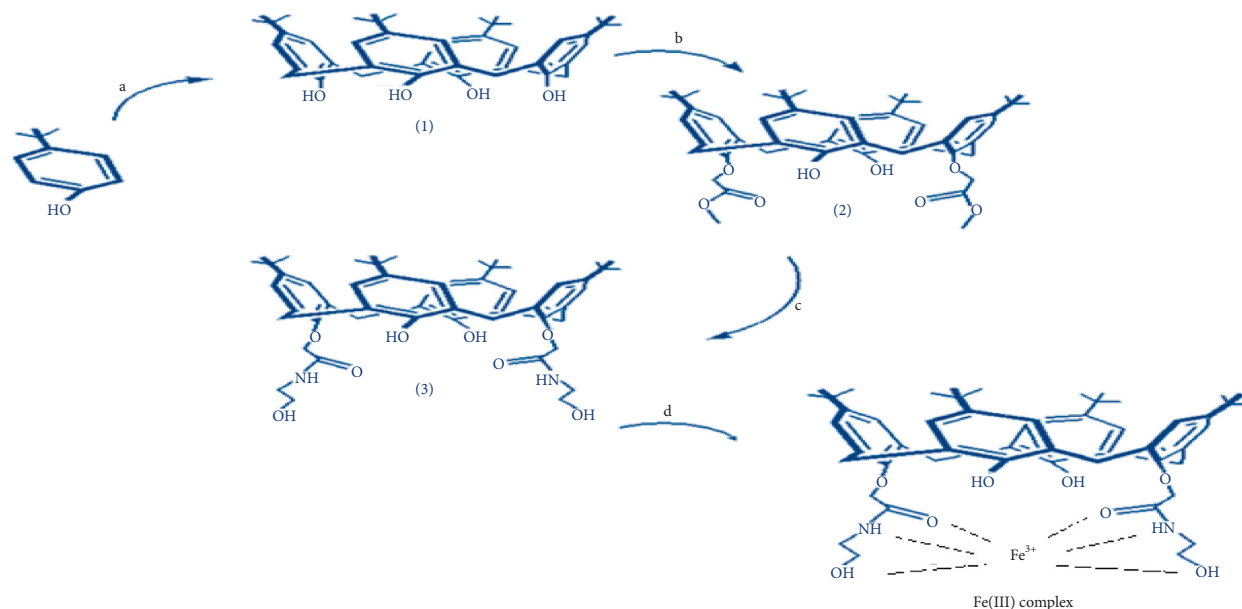
FIGURE 1: Experimental scheme for the synthesis of 1–3 and Fe^{3+} complex of **3** (derivative L). The conditions specified for each step are (a) $HCHO/NaOH$, (b) $KCO_3/C_4H_7BrO_2$, (c) C_2H_7NO/CH_3OH, and (d) $FeCl_3 \cdot 6H_2O$, respectively.

3. Results and Discussion

3.1. UV-Vis Study. UV-Vis spectroscopic technique was used to explore the complexation behavior of the derivative (L) against various essential metal ions, i.e., K^+, Na^+, Mg^{2+}, Fe^{3+}, Co^{2+}, Zn^{2+}, and Ni^{2+}. 10 eq. of various metal ions was used against the derivative (L) $(2.6 \times 10^{-3}\,M)$ in absolute ethanol to check the complexation ability. Figure 2 shows the UV-Vis spectra of the derivative (L) after the addition of metal ions.

The result showed the prominent variations in peaks during complexation. The obtained spectra showed that the derivative (L) possesses good attraction towards the essential metal ions (showing the difference in region 220–230 nm), but it showed noticeable interaction to Fe^{3+}.

The electronic spectra of the derivative (L), Fe^{3+}, and Fe^{3+} complex were recorded in ethanol, as given in Figure 3, and values of wavelength maximum are given in Table 1. The reported complex is novel having brownish color. Actually, the transition metals having incomplete d orbital absorb radiation in the UV-Vis region and show electronic transitions between different energy levels, whose separation is largely controlled by ligand species. The spectrum observed in Figure 3 for the derivative (L) indicates that 215 and 280 nm peaks are produced by intraligand transitions. In case of the Fe^{3+} complex, red shifts were observed. In the complex, peaks observed at 250 and 300 nm are assigned to characteristic metal d-d transitions. It indicates that metal and ligand molecules are well incorporated to give observed spectral changes. Likewise, when metal and ligand are coordinated, ligand causes splitting within d orbitals of metal shifting it to longer wavelength. Spectrum of ligand has shown a bathochromic shift after coordination.

Iron gives octahedral geometry here because it produces six coordination environments. Since Fe^{3+} gives the d^5
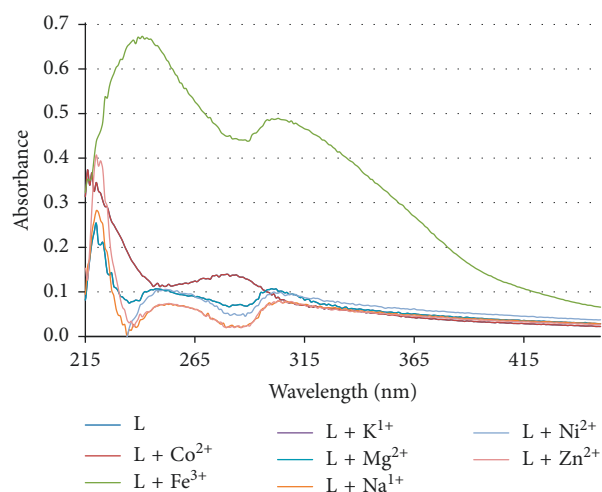

FIGURE 2: Absorption spectra of the derivative L (ligand) $(2.6 \times 10^{-5}\,M)$ with different essential metals ions $(2.6 \times 10^{-4}\,M)$.

system, whereas Fe^{2+} gives d^6, the high charge density and small size of Fe^{3+} make it a hard base, where O and N donor ligands appear to be small sized, and relatively non-polarisable ligands are hard bases; hence, this type of hard-hard type acid-base combination favors significantly stable Fe^{3+} derivative (L) complex, whereas Fe^{2+} is classified as borderline acid which will probably give less stable complex. The complex has faint brownish color mostly due to the d-d transition that gives weak colors since it is a Laporte forbidden transition. However, transitions after complex formation may involve electronic rearrangements of valence electrons. Moreover, complex color is mostly dependent on metal, oxidation state of metal, and number of d electrons in metal, as Fe^{2+} gives green color, while Fe^{3+} produces brown color. Contrary to this, charge transfer is less probable here
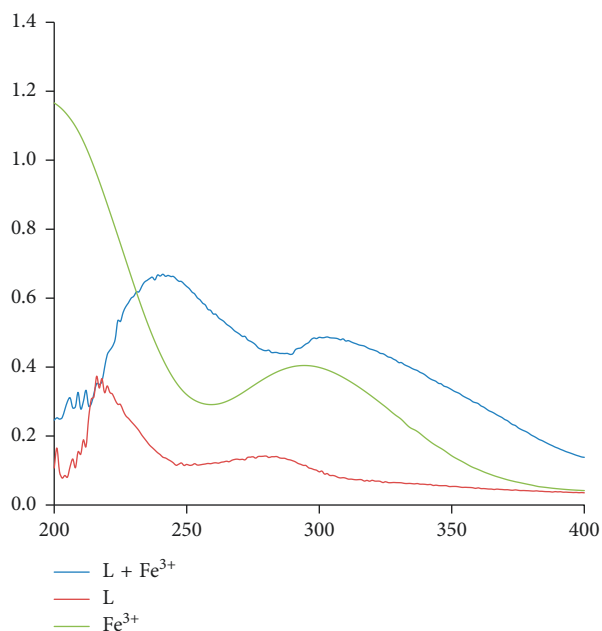
FIGURE 3: UV-Vis spectra of ligand (L), Fe^{3+}, and Fe^{3+} complex.

TABLE 1: λ_{max} of various transitions in the derivative (L) and iron complex.

Compounds	Transitions (λ in nm)	
Derivative (**L**)	215	280
L-Fe^{3+} complex	250	300

because internally it involves the oxidation-reduction process. LMCT and MLCT cause the redox changes and may give very strong/sharp peaks. Such change is not observed here, but instead weak peaks are observed here evidencing the peaks to be produced from d-d transitions. However, it is believed that variation in absorption peaks is associated with stable chelate complex formation in case of iron, which further supported the complexation. Furthermore, the study was carried out on the Fe^{3+} complex.

3.2. Concentration Study.

In order to evaluate the complexation efficiency of the derivative (L), the concentration of Fe^{3+} was steady increased from 1.0 to 10 equivalents. The results shown in Figure 4 indicate that adsorption intensity of the derivative (L) was increased linearly with the increasing dose of Fe^{3+} ions. These results suggest that derivative (L) possesses appreciable binding efficiency with Fe^{3+}.

3.3. Job's Plot for Fe^{3+} Complex.

Technique of constant variation was performed for Job's plot using absorbance versus mole fraction (X) to know the stoichiometric ratio between the derivative (L) and Fe^{3+} metal ion. In case of Job's plot study for the Fe^{3+} complex, it is revealed that derivative (L) shows good complexation at 0.5 mole fraction (Figure 5), which reflects that derivative (L) and Fe^{3+} possesses good relation in 1 : 1. Therefore, the reaction was set
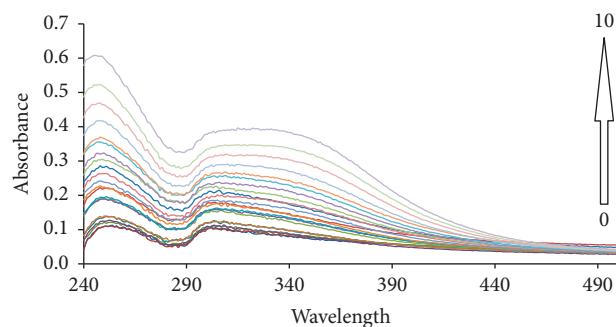

FIGURE 4: UV-Vis titration spectra of derivative (L) (2.6×10^{-5} M) by adding various equivalents (0–10 eq.) of Fe^{3+}.
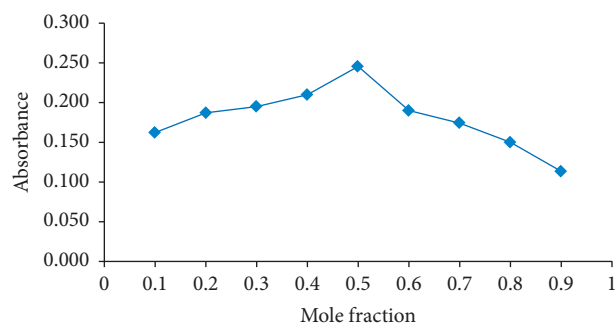

FIGURE 5: Job's plot produced by mixing various equivalents of the derivative (L) (2.6×10^{-5}) and Fe^{3+} (2.6×10^{-5}).

between derivative (L) and Fe^{3+} in absolute ethanol using indicated appropriate ratios for complex synthesis.

3.4. Characterization of Fe^{3+} Complex.

FT-IR study helps to confirm the complex formation by showing disappearance and appearance or shifting of some peaks present in the derivative (L) spectrum after complexation. Figure 6 shows the comparable spectra of the derivative (L) and its Fe^{3+} complex in which reasonable changes are observed. A band 1666.49 cm^{-1} for C=O is shifted to 1659.76 cm^{-1} in the Fe^{3+} complex spectrum. Also a band 1549.27 cm^{-1} for NH bending is shifted to 1541.39 cm^{-1} after complexation. Two peaks at 1110.4 cm^{-1} and 1059.34 cm^{-1} for C-O stretch of hydroxyl of the ethanolamine group are shifted to 1104.2 cm^{-1} and 1051.6 cm^{-1} after complexation. The OH stretch peak at 3382.99 cm^{-1} is also shifted to 3378.9 cm^{-1} on complexation with Fe^{3+}. These remarkable changes suggest that Fe^{3+} coordinates with nitrogen, oxygen of the carbonyl group, and oxygen of the hydroxyl group. In addition, these changes indicate the complex formation.

Elemental analysis found (%): C, 73.36; H, 8.20; N, 3.35. Anal. Calcd for compound **3** (%): C, 73.41: H, 8.24: N, 3.39. Similarly elemental analysis found (%): C, 68.91; H, 7.7; N, 3.06. Anal. Calcd for Fe complex (%): C, 68.95; H, 7.7; N: 3.09.

3.5. Antimicrobial Study.

Derivative (L) and its Fe^{3+} complex are good antimicrobial agents, as shown in Tables 2 and 3.
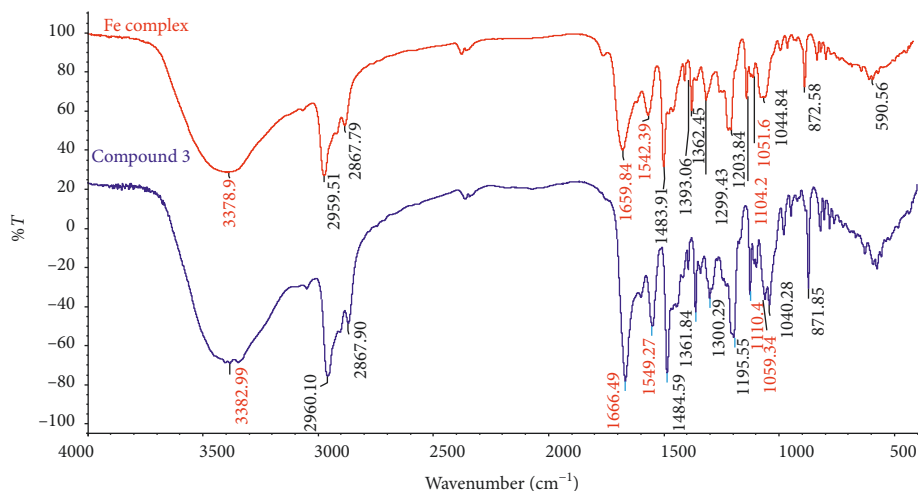
FIGURE 6: FT-IR spectra of compound 3 (L) and its complex with Fe^{3+}.

TABLE 2: Zones of inhibition for antimicrobial activities of the tested derivative (L).

Microorganism strains	Derivative (L) (concentration in μg/mL)					MIC value (μg/mL)
	6	3	1.5	0.75	0.37	
	(zones of inhibition in mm)					
S. albus	6	2	—	—	—	3
E. coli	8	3	—	—	—	3
R. stolonifer	9	4	1	—	—	1.5

TABLE 3: Zones of inhibition for antimicrobial activities of the tested Fe^{3+} complex of the derivative (L).

Microorganism strains	Fe^{3+} complex (concentration in μg/mL)					MIC value (μg/mL)
	6	3	1.5	0.75	0.37	
	(zones of inhibition in mm)					
S. albus	13	10	6	4	2	0.37
E. coli	17	15	12	8	3	0.37
R. stolonifer	15	12	9	3	1	0.37

They showed antimicrobial activity against selected microorganisms (S. albus, E. coli, and R. stolonifer). However, it is important to note that the Fe^{3+} complex showed higher antimicrobial activity as compared to the derivative (L). Increase in the activity of complex can be explained on the basis of Tweedy's chelating theory [22] and overtone concept [23, 24]. A preliminary evaluation of the antimicrobial activity of the derivative (L) and Fe^{3+} complex against S. albus and E. coli was performed and gauged according to the following four stage criteria:

(+++) High antimicrobial activity; zone of inhibition is 12–17 mm

(++) Relatively high antimicrobial activity; zone of inhibition is 8–11 mm

(+) Weak antimicrobial activity; zone of inhibition is 1–7 mm

(−) No antimicrobial activity

3.6. Antibacterial Activity. From Figures 7 and 8, it is clear that the Fe^{3+} complex showed higher antimicrobial activity (+++) at 6 μg/mL against S. albus, and for E. coli, it showed higher antimicrobial activity (+++) at 6, 3, and 1.5 μg/mL, while it showed relatively high antimicrobial activity (++) at 3 μg/mL against S. albus and at 0.75 μg/mL against E. coli. It showed weak antimicrobial activity (+) below 3 μg/mL against S. albus and at 0.37 μg/mL against E. coli. However, derivative (L) showed relatively high antimicrobial activity (++) at 6 μg/mL and weak antimicrobial activity (+) at 3 μg/mL against E. coli. It showed weak antimicrobial activity (+) at 6 and 3 μg/mL against S. albus. No antimicrobial study (−) was observed below 3 μg/mL for both bacterial strains.

3.7. Antifungal Activity. Antifungal activity of the derivative (L) and its Fe^{3+} complex was carried out against R. stolonifer. Figure 9 shows that the Fe^{3+} complex showed higher an-
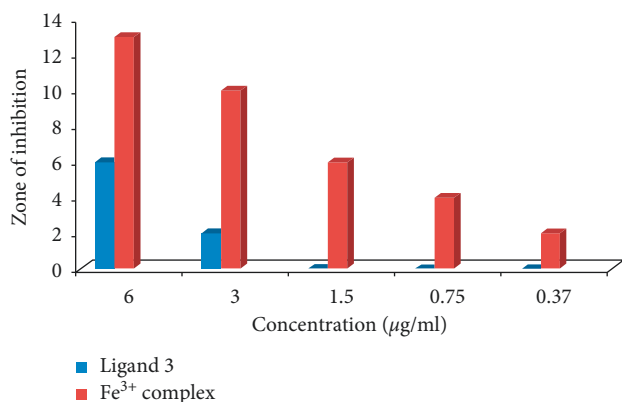
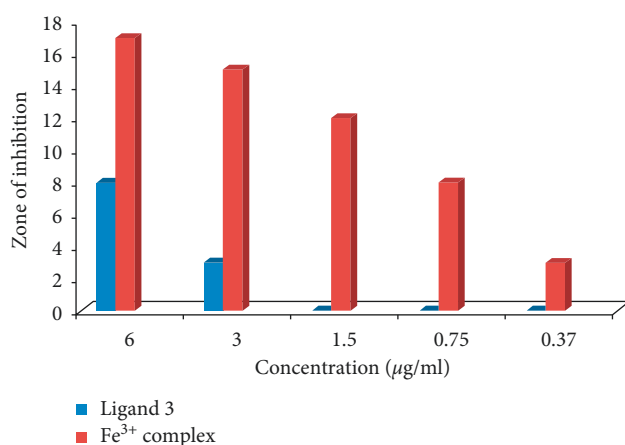FIGURE 7: Antimicrobial activity of ligand **3 (L)** and its Fe^{3+} complex against *S. albus* (G +ve).

FIGURE 8: Antimicrobial activity of the derivative (L) and its Fe^{3+} complex against *E. coli* (G −ve).

FIGURE 9: Antifungal activity of ligand **3 (L)** and its Fe^{3+} complex against *R. stolonifer* (fungus) concentration (μg/mL).

FIGURE 10: MIC values of ligand **3 (L)** and its metal complex against *S. albus* (G +ve).

FIGURE 11: MIC values of ligand **3 (L)** and its metal complex against *E. coli* (G -ve).

timicrobial activity (+++) at 6 and 3 μg/mL, relatively high antimicrobial activity (++) at 1.5 μg/mL, and weak antimicrobial activity (+) at 0.75 and 0.37 μg/mL. However, derivative (L) showed no higher antimicrobial activity but relatively high antimicrobial activity (++) at 6 μg/mL and weak antimicrobial activity (+) at 3 and 1.5 μg/mL against *R. stolonifer*.

3.8. Minimum Inhibitory Concentration (MIC). The minimum concentration at which the growth of microorganisms (bacteria and fungi) is inhibited is usually known as *in vitro* minimum inhibitory concentration (MIC) [25]. Different concentration level solutions (6, 3, 1.5, 0.75, and 0.37 μg mL^{-1}) of the derivative (L) and its metal complex were prepared against bacteria and fungi (Tables 2 and 3). Figures 10 and 11 show that derivative (L) had the same MIC values (3 μg/mL) for both selected bacterial strains, which means it is less effective against bacteria because at lower concentrations, its effect was not observed. However, the Fe^{3+} complex showed high activity against *E. coli* and *S. albus* with an MIC value of 0.37 μg/mL for both bacteria, because it showed antimicrobial action even at lower concentrations. Thus, the Fe complex of the derivative (L)
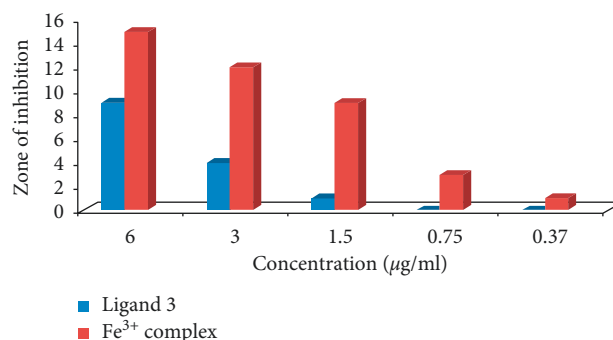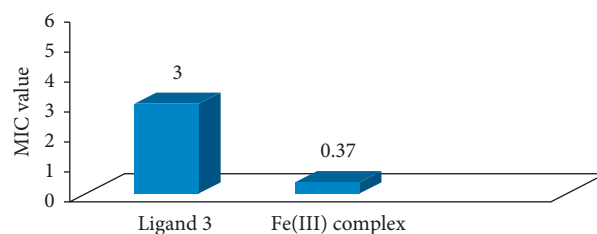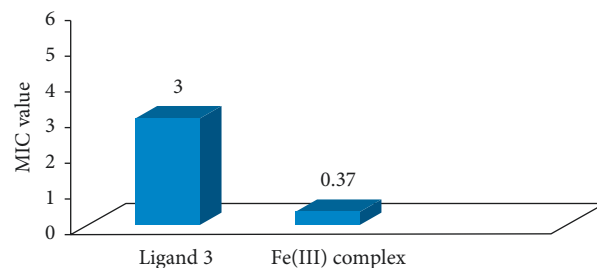
synthesized in this study is the most potent antimicrobial agent than calix[4]arene derivative reported so far such as calix[4]arene-based vancomycin mimics [11], antibacterial *tetra-para*-guanidinoethyl-calix[4]arenes [26], water-soluble nalidixic acid/calix [4]arene ester adducts [27], and water-soluble calix[4]arenes derivatives [6].

In case of antifungal action, Figure 12 shows that derivative (L) had an MIC value of 1.5 μg/mL, which means it is more effective against *R. stolonifer* as compared to selected bacteria for which it showed an MIC value of 3 μg/mL. However, the Fe^{3+} complex was equally effective against the fungi and two bacterial species tested with an MIC value of 0.37 μg/mL.

4. Conclusions

The derivative (L) was synthesized and explored for the complexation study with essential metals. It was revealed that derivative (L) showed selective behavior toward the Fe^{3+} ion. Job's plot study evaluated that derivative (L) and Fe^{3+}
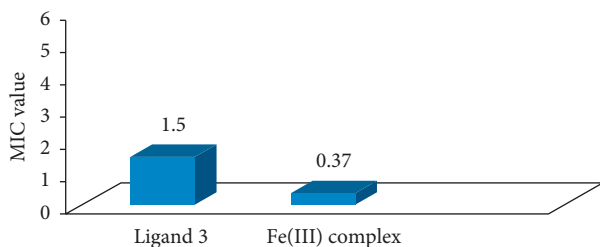
FIGURE 12: MIC values of ligand **3 (L)** and its metal complex against *R. stolonifer*.

metal ion form good complex in 1 : 1 ratio. Finally, derivative (L) and its Fe^{3+} complex were bioassayed for antimicrobial activity. On the basis of MIC values, it is concluded that the Fe^{3+} complex of the derivative (L) is more effective against selected bacteria and fungi, as compared to the derivative (L) because the Fe^{3+} complex showed higher antimicrobial sensitivity towards selected bacteria and fungi by showing an MIC value of 0.37 μg/mL. Thus, the Fe^{3+} complex of the derivative (L) may prove to be a good candidate for further studies as a pharmaceutical drug.

Data Availability

All the data relevant to the study are present in this article.

Disclosure

Conflicts of Interest

The authors declare that there are no conflicts of interest.

Acknowledgments

References

[1] C. D. Gutsche and L.-G. Lin, "Calixarenes 12," *Tetrahedron*, vol. 42, no. 6, pp. 1633–1640, 1986.

[2] M. Yilmaz and S. Sayin, "Calixarenes in organo and biomimetic catalysis," in *Calixarenes and Beyond*, pp. 719–742, Springer, Cham, Switzerland, 2016.

[3] J. S. Kim and D. T. Quang, "Calixarene-derived fluorescent probes," *Chemical Reviews*, vol. 107, no. 9, pp. 3780–3799, 2007.

[4] C. Redshaw, "Coordination chemistry of the larger calixarenes," *Coordination Chemistry Reviews*, vol. 244, no. 1-2, pp. 45–70, 2003.

[5] M. Yigiter Bayrakcı, S. Ertul, and M. Yilmaz, "Synthesis of novel silica gel immobilized-calix4arene amide ionophores and their anion binding abilities toward phosphate and chromate anions," *Journal of Applied Polymer Science*, vol. 124, no. 5, pp. 3831–3839, 2012.

[6] A. M. Soomro, R. K. Oad, S. Memon, and I. Qureshi, "Pak. Bioactivity assessment of water soluble calix[4]arene derivative," *Pakistan Journal of Analytical and Environmental Chemistry*, vol. 13, pp. 36–39, 2012.

[7] J. S. Millership, "A preliminary investigation of the solution complexation of 4-sulphonic calix[n]arenes with testosterone," *Journal of Inclusion Phenomena and Macrocyclic Chemistry*, vol. 39, no. 3/4, pp. 327–331, 2001.

[8] E. D. Silva, P. Shahgaldian, and A. W. Coleman, "Haemolytic properties of some water-soluble para-sulphonato-calix-[n]-arenes," *International Journal of Pharmaceutics*, vol. 273, pp. 57–62, 2004.

[9] J. Gualbert, P. Shahgaldian, and A. W. Coleman, "Interactions of amphiphilic calix[4]arene-based Solid Lipid Nanoparticles with bovine serum albumin," *International Journal of Pharmaceutics*, vol. 257, no. 1-2, pp. 69–73, 2003.

[10] J. W. Conforth, P. D. Hart, G. A. Nicholls, R. J. W. Rees, and J. A. Stock, "Antituberculous effects of certain surface-active polyoxyethylene ethers," *British Journal of Pharmacology and Chemotherapy*, vol. 10, no. 1, pp. 73–86, 1955.

[11] A. Casnati, M. Fabbi, N. Pelizzi et al., "Synthesis, antimicrobial activity and binding properties of calix[4]arene based vancomycin mimics," *Bioorganic and Medicinal Chemistry Letters*, vol. 6, no. 22, pp. 2699–2704, 1996.

[12] V. Paquet, A. Zumbuehl, and E. M. Carreira, "Biologically active amphotericin B-Calix[4]arene conjugates," *Bioconjugate Chemistry*, vol. 17, no. 6, pp. 1460–1463, 2006.

[13] R. Lamartine, M. Tsukada, D. Wilson, and A. Shirata, "Antimicrobial activity of calixarenes," *Comptes Rendus Chimie*, vol. 5, no. 3, pp. 163–169, 2002.

[14] Ş. Ç. Özkan, A. Yilmaz, E. Arslan, L. Açık, Ü. Mutlu, and E. G. Elif, "Novel copper(II) complexes ofp-tert-butylcalix[4] arene diamide derivatives: synthesis, antimicrobial and DNA cleavage activities," *Supramolecular Chemistry*, vol. 27, no. 4, pp. 255–267, 2015.

[15] C. D. Gutsche, M. Iqbal, and D. Stewart, "Calixarenes. 19. Syntheses procedures for p-tert-butylcalix[4]arene," *Journal of Organic Chemistry*, vol. 51, no. 5, pp. 742–745, 1986.

[16] D. Maity, A. Chakraborty, R. Gunupuru, and P. Paul, "Calix [4]arene based molecular sensors with pyrene as fluorogenic unit: effect of solvent in ion selectivity and colorimetric detection of fluoride," *Inorganica Chimica Acta*, vol. 372, no. 1, pp. 126–135, 2011.

[17] S. Inese and D. B. Smithrud, "Condensation of calix[4]arenes with unprotected hydroxyamines and their resulting water solubilities," *Tetrahedron*, vol. 57, no. 47, pp. 9555–9561, 2001.

[18] D. C. Harris, *Quantitative Chemical Analysis*, Vol. 4, W.H. Freeman and Company, New York, NY, USA, 1995.

[19] Q. K. Panhwar, S. Memon, and M. I. Bhanger, "Synthesis, characterization, spectroscopic and antioxidation studies of Cu(II)-morin complex," *Journal of Molecular Structure*, vol. 967, no. 1–3, pp. 47–53, 2010.

[20] A. W. Bauer, W. M. A. Kirby, J. C. Sherris, and M. Truck, "Antibiotic susceptibility testing by a standardized single disk method," *American Journal of Clinical Pathology*, vol. 45, pp. 493–496, 1996.

[21] D. A. V. Berghe and A. J. Vlietinck, "Screening methods for antibacterial and antiviral agents from higher plants," in *Meth. Plant Biochem.*, P. M. Dey and J. D. Harbone and, Eds., p. 47, Academic Press, London, UK, Academic Press, 1991.

[22] J. Joseph, K. Nagashri, and G. A. B. Rani, "Synthesis, characterization and antimicrobial activities of copper complexes

derived from 4-aminoantipyrine derivatives," *Journal of Saudi Chemical Society*, vol. 17, no. 3, pp. 285–294, 2013.

[23] S. A. Sadeek, W. H. El–Shwiniy, W. A. Zordok, and A. M. El-Didamony, "Synthesis, spectroscopic, thermal and biological activity investigation of new Y(III) and Pd(II) Norfloxacin complexes," *Journal of the Argentine Chemical Society*, vol. 97, pp. 128–148, 2009.

[24] Q. K. Panhwar and S. Memon, "Synthesis, characterization and microbial evaluation of metal complexes of molybdenum with ofloxacin (levo (S-form) and dextro (R-form)) isomers," *Journal of Modern Medicinal Chemistry*, vol. 2, pp. 1–9, 2014.

[25] F. Mojab, M. Poursaeed, Mehrgan, and S. Pakdaman, "Antibacterial activity of Thymus daenensis methanolic extract," *Pakistan Journal of Pharmaceutical Sciences*, vol. 21, pp. 210–213, 2008.

[26] M. Mourer, R. E. Duval, C. Finance, and J.-B. Regnouf-de-Vains, "Functional organisation and gain of activity: the case of the antibacterial tetra-para-guanidinoethyl-calix[4]arene," *Bioorganic and Medicinal Chemistry Letters*, vol. 16, no. 11, pp. 2960–2963, 2006.

[27] H. M. Dibama, I. Clarot, S. Fontanay et al., "Towards calixarene-based prodrugs: drug release and antibacterial behaviour of a water-soluble nalidixic acid/calix[4]arene ester adduct," *Bioorganic and Medicinal Chemistry Letters*, vol. 19, no. 10, pp. 2679–2682, 2009.